

# Improved power quality converter for direct torque control-based induction motor drives

Sandeep Madishetti, G. Bhuvaneshwari, Bhim Singh

Department of Electrical Engineering, Indian Institute of Technology Delhi, New Delhi-110016, India  
E-mail: sandeep.madishetti@gmail.com

**Abstract:** This study presents the performance of a direct torque control (DTC)-based induction motor drive (IMD) with improved power quality converter at the front end. It is designed, modelled, simulated in MATLAB/simulink platform and implemented in hardware using a digital signal processor (DSP). An improved power quality converter known as Vienna rectifier is used in the system to mitigate the power quality problems at the utility interface in the DTC-IMD. The proposed Vienna rectifier is a three switch converter to improve the power quality in terms of reduced total harmonic distortion of ac mains current, power factor correction and dc-link voltage regulation. The performance of the proposed system is validated experimentally using a DSP. The performance of the system is tested for step change in input reference speed and the load torque and it is found that the power quality indices conform to IEEE-519 standard under all operating conditions.

## 1 Introduction

Direct torque control (DTC) of induction motor drives (IMD) has become an industry standard control because of its advantages like ease of control, absence of co-ordinate transformations, independence from machine parameters, flux and torque proportional-integral-derivative (PID) controllers being absent, requirement for neither a separate PWM block and nor the exact determination of flux vector position. DTC as the name implies controls directly the stator (or rotor/magnetising) flux and electromagnetic torque by the selection of optimum inverter switching modes. The selection of switching is made in such way as to restrict the flux and torque errors within respective flux and torque hysteresis bands to obtain fast torque response, low inverter switching frequency and low harmonics. In DTC, the torque and flux are directly controlled without any PWM modulators and co-ordinate transformations and hence the response of the drive is much faster than the field-oriented control (FOC) technique especially to load torque and reference speed variations.

Conventional DTC drives are generally fed from a six-pulse un-controlled diode bridge rectifier (DBR) at the front end for converting input three-phase ac mains voltages into dc voltage; a capacitor filter is used at the output of the rectifier for smoothing the dc-link voltage. A voltage source inverter (VSI) converts this dc to a variable frequency ac, which drives the three-phase induction motor. Because of the presence of un-controlled bridge rectifier and capacitor filter at the front end, it draws a non-sinusoidal current from the grid [1]. This causes injection of harmonic currents into the ac mains, poor power factor, equipment overheating because of harmonics current absorption, variation in dc-link voltage with

fluctuations in the voltage of input ac supply, voltage distortion at the point of common coupling (PCC) because of the voltage drop caused by harmonics current flowing through system impedance, interference in telephone and communication lines and decreased rectifier efficiency. Different international standards such as IEEE-519 and IEC 61000-3-2 specify guidelines to impose strict limits on the levels of harmonics current and voltage emissions.

Casadei *et al.* [2] have compared two different control techniques namely FOC and DTC of IMD. This paper clearly explains the advantages of DTC over FOC. Different active wave shaping techniques are used for improving the power quality at the front end of DTC-based IMD. Domijan *et al.* [3] have presented some harmonic mitigation techniques for the improvement of power quality of adjustable speed drives. Singh *et al.* [4] have presented a comprehensive survey on three-phase ac-dc converters with improved power quality in terms of power-factor correction, reduced total harmonic distortion (THD) at input ac mains, and regulated dc output voltage. Kolar *et al.* [5] have explained the development of guidelines for the practical application of a new power module realising a bridge leg of application of a three-phase/switch/level PWM (Vienna) rectifier system with low deteriorating effects on the ac mains. Kolar *et al.* [6] have analysed the stationary operational behaviour, the control of the ac mains currents and the output voltage of Vienna rectifier for telecommunication applications. This paper also compares the stresses on the system components of Vienna rectifier with the conventional PWM rectifier system. Dalessandro *et al.* [7] have proposed a novel hysteresis current controller for Vienna rectifier which allows a full utilisation of the modulation range and an intrinsic stability of the output centre point voltage. On the other hand, Youssef *et al.* [8]

have presented a new small-signal-modelling technique and validation procedure applied to a three-phase three-level boost-type AC/DC Vienna converter. Naik *et al* [9] have proposed an improved power quality converter using two switches for dc bus regulation and to minimise the line-current harmonics.

This paper mainly focuses on the performance comparison of two front end converters for a DTC-based IMD namely – a conventional six-pulse DBR and an improved power quality converter (Vienna rectifier). It shows how the power quality can be improved significantly at the utility interface by making use of this improved power quality rectifier. The advantageous features of Vienna rectifier as the front end converter for the DTC-based IMD as compared with a six-switch PWM controlled rectifier are (i) only three switches used, (ii) semi-conductor blocking voltage is reduced to 50% (iii) dead short-circuit of dc-link does not occur even if the control is faulty which guarantees high reliability. As the blocking voltage of semi-conductor switches in Vienna rectifier is less, switching losses are reduced and hence it is more efficient than the PWM rectifier and the size of the heat sink reduces. Simple control scheme is utilised to stabilise the neutral point potential in Vienna rectifier. The three-level characteristics in Vienna rectifier reduces input-current ripple and input inductor volume for a specified ripple content, as compared with two-level PWM rectifier. Since Vienna rectifier is a unidirectional converter, this is used in such motor drive applications such as heating, blowers, fans and air-conditioning, where regenerative braking is not mandatory. The organisation of the paper is as follows: first, it describes power quality issues with conventional six-pulse DBR-fed DTC-based IMD; then, it presents the system configuration of Vienna rectifier for improving the power quality. Further, modelling of the DTC-based IMD with Vienna rectifier is described in detail. The performance of Vienna rectifier-fed DTC-based IMD is analysed for different reference speed settings and load torque

perturbations. Harmonic analysis of ac mains current of the drive system is carried out for different loading conditions. The performance of the proposed drive system is analysed for non-ideal ac mains voltages (un-balanced and distorted). The prototype of the proposed drive system is implemented using Texas Instruments digital signal processor (DSP) and the experimental results have also been presented for speed and load torque variations on the DTC-based IMD.

## 2 System configuration and principle of operation

An improved power quality converter namely Vienna rectifier is used for eliminating ac mains current harmonics at the front end of the DTC-based three-phase IMD. Fig. 1 shows the system configuration of DTC-based IMD with a Vienna rectifier.

A Vienna rectifier is a three-phase, three-switch, three-level boost type PWM rectifier used for reducing the harmonics in ac mains currents, improving the power factor and regulating the dc-link of a DTC drive. The power circuit of the Vienna rectifier is shown in Fig. 1. Each leg of the Vienna rectifier consists of a bi-directional switch which is realised by connecting an MOSFET (metal-oxide-semiconductor field-effect transistor) across the dc terminals of a DBR and two free-wheeling diodes. It provides sinusoidal input currents and controlled dc-voltage if appropriately controlled. The energy cannot be fed back to the ac mains by using this converter. So, where the drive applications do not require regeneration, Vienna rectifier seems to be a suitable solution for improving the power quality with unity power factor (UPF) operation at the ac mains.

### 2.1 Control algorithm

The control algorithm for the proposed drive system is mainly divided into two parts. The Vienna rectifier controller

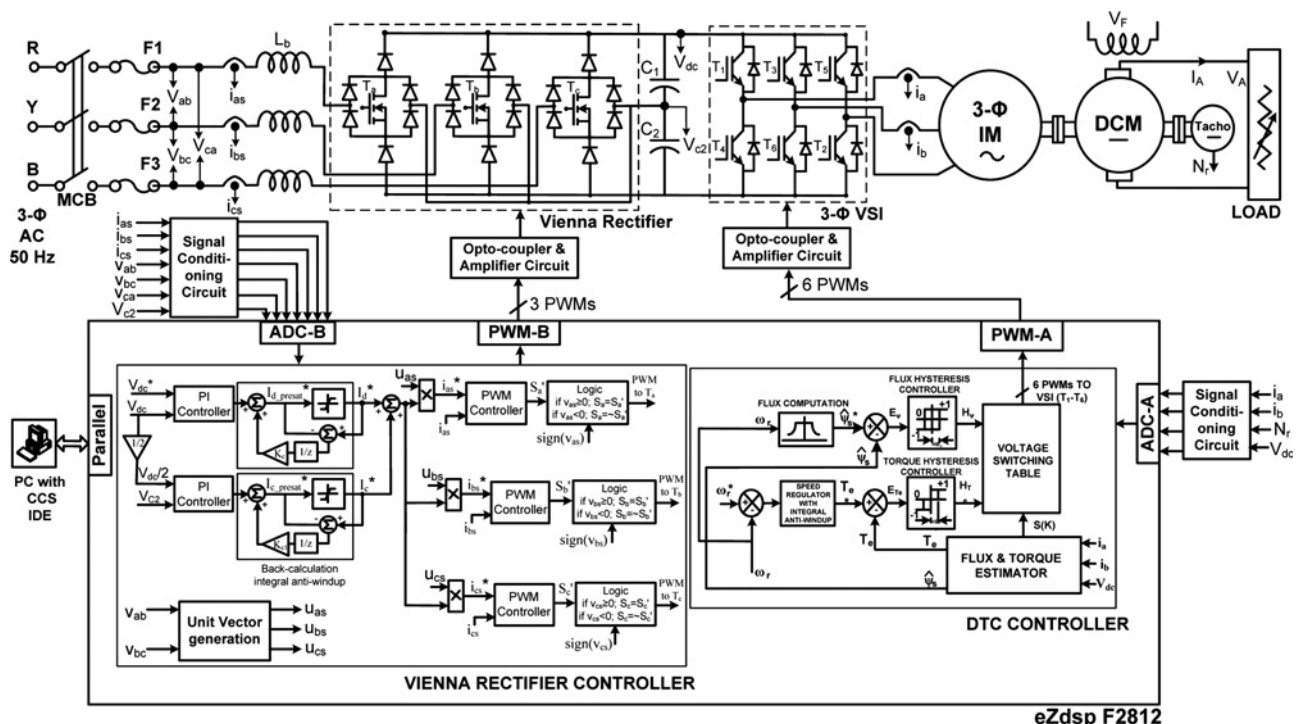


Fig. 1 System configuration of DTC-based IMD with Vienna rectifier

generates three PWM pulses for its devices and DTC control algorithm generates six PWM pulses for the VSI which drives three-phase induction motor. The modelling of these controllers used for implementation of the proposed system is as follows.

**2.1.1 Vienna rectifier:** The block diagram of the controller for generating PWM signals to the switches of the Vienna rectifier is shown in Fig. 1. It contains one inner current control loop and an outer voltage control loop.

The modelling of the controller is done as follows: The sensed dc-link voltage  $V_{dc}$  is compared with the reference dc-link voltage  $V_{dc}^*$  to generate  $I_d^*$  through a proportional plus integral (PI) voltage controller

$$I_{d(n)}^* = I_{d(n-1)}^* + K_p (V_{dc\_e(n)} - V_{dc\_e(n-1)}) + K_i V_{dc\_e(n)} \quad (1)$$

where  $I_{d(n)}^*$ ,  $I_{d(n-1)}^*$  are the output of the PI dc-link voltage controller at  $n$ th and  $(n-1)$ th steps; and  $V_{dc\_e(n)}$ ,  $V_{dc\_e(n-1)}$  are the errors of the dc-link voltage at the  $n$ th and  $(n-1)$ th instants;  $K_p$  and  $K_i$  are the proportional and integral controller constants. The  $K_p$  and  $K_i$  values are found by using Ziegler Nichols method. Initially  $K_i$  is set to 0 and  $K_p$  is increased slowly until the response starts to oscillate. This proportional gain is  $K_u$  and the period of oscillation is considered to be  $T_u$ .  $K_p$  and  $K_i$  are estimated as  $K_p = 0.45K_u$  and  $K_i = 1.2K_p/T_u$ . After estimating  $K_p$  and  $K_i$  values from this method, these values are fine tuned according to desired response for less settling time and near zero steady state error. The integral wind-up is taken care of by using back-calculation algorithm. In this method, when the PI controller output saturates, the integral term in the controller is recomputed so that its new value gives an output within the saturation limit.

The block diagram of this method is shown in Fig. 1. Equation (1) is modified as given below as per Fig. 1.

$$I_{d(n)}^* = I_{d(n-1)}^* + K_p \left\{ V_{dc\_e(n)} - V_{dc\_e(n-1)} \right\} + K_i V_{dc\_e(n)} + K_c \left\{ I_{d(n-1)}^* - I_{d\_presat(n-1)}^* \right\} \quad (2)$$

$$I_{d(n)}^* = \text{sat} \left( I_{d\_presat(n)}^* \right) \quad (3)$$

The difference in two capacitors voltages ( $V_{c1}$  and  $V_{c2}$ ) is compensated by generation of reference current  $I_c^*$  to make equal voltages across dc bus capacitors  $C_1$  and  $C_2$  using a PI controller as

$$I_{c(n)}^* = I_{c(n-1)}^* + K_{p1} \left\{ V_{c\_e(n)} - V_{c\_e(n-1)} \right\} + K_{i1} V_{c\_e(n)} \quad (4)$$

where  $I_{c(n)}^*$ ,  $I_{c(n-1)}^*$  are the output of the PI controller at the two instants  $n$  and  $(n-1)$ ; and  $V_{c\_e(n)}$ ,  $V_{c\_e(n-1)}$  are the errors between half of dc-link voltage and  $V_{c2}$  ( $V_{c\_e} = V_{dc}/2 - V_{c2}$ ) at the  $n$ th and  $(n-1)$ th instants;  $K_{p1}$  and  $K_{i1}$  are the proportional and integral controller constants. Similarly, tuning of  $K_{p1}$  and  $K_{i1}$  are done using Ziegler Nichols method as mentioned above. The integral anti-windup is taken care by back-calculation method.

$I_{dc}^*$  and  $I_c^*$  are added and then multiplied with unit templates ( $u_{as}$ ,  $u_{bs}$ ,  $u_{cs}$ ) of fundamental positive sequence phase voltages ( $v_{as}$ ,  $v_{bs}$ ,  $v_{cs}$ ) and added with  $I_c^*$  to generate

reference line currents ( $i_{as}^*$ ,  $i_{bs}^*$ ,  $i_{cs}^*$ ).

$$i_{as}^* = u_{as} (I_{dc}^* + I_c^*) \quad (5)$$

The unit template voltages are generated by using the sensed ac mains line-line voltages ( $v_{ab}$ ,  $v_{bc}$  and  $v_{ca}$ ). If the ac mains voltages are distorted and un-balanced, they will have harmonics and negative sequence component. First, fundamental line-line voltages ( $v_{ab1}$ ,  $v_{bc1}$  and  $v_{ca1}$ ) are extracted from sensed line-line voltages ( $v_{ab}$ ,  $v_{bc}$  and  $v_{ca}$ ) and then positive sequence voltages ( $v_{ab1}^+$ ,  $v_{bc1}^+$  and  $v_{ca1}^+$ ) are computed from therein. The fundamental positive sequence phase voltages ( $v_{as1}^+$ ,  $v_{bs1}^+$  and  $v_{cs1}^+$ ) of the ac mains are extracted from the fundamental positive sequence line-line voltages ( $v_{ab1}^+$ ,  $v_{bc1}^+$  and  $v_{ca1}^+$ ). Then voltage unit templates are calculated as

$$u_{as} = v_{as1}^+ / V_t, u_{bs} = v_{bs1}^+ / V_t \text{ and } u_{cs} = v_{cs1}^+ / V_t \quad (6)$$

where  $V_t$  is amplitude of terminal voltage of the fundamental positive sequence phase voltages.

The reference phase current ( $i_{as}^*$ ) and actual phase current ( $i_{as}$ ) are compared and the current error ( $\Delta i_{as}$ ) is amplified by multiplying it by a constant gain ( $K$ ); then the amplified error ( $K\Delta i_{as}$ ) is compared with modulating triangular waveform  $m_{tria}$  to generate PWM pulse  $S'_a$ .

If  $K\Delta i_{as} \geq m_{tria}$ ;  $S'_a = 1$ , else  $S'_a = 0$ .

The sign of the phase voltage  $v_{as}$  is taken into account when making a switching decision  $S_a$ , this can be realised by using exclusive OR (XOR) gate as shown in Vienna rectifier controller block diagram (Fig. 1). The output of XOR gate ( $S_a$ ) is given to the MOSFET  $T_a$

$$S_a = S'_a; \text{ if } v_{as} \geq 0 \quad (7)$$

$$S_a = \tilde{S}'_a; \text{ if } v_{as} < 0 \quad (8)$$

Similarly, the PWM signals for MOSFETs  $T_b$  and  $T_c$  are generated using above procedure as shown in Fig. 1.

**2.1.2 DTC-based IM drive:** DTC of an IMD offers a better dynamic response than the FOC technique because of direct control of flux and torque independent of each other. The control is implemented using mainly three blocks [10]: flux and torque hysteresis controller, voltage switching table and flux, torque and speed estimators as shown in Fig. 1 (DTC controller). In this control, the torque and stator flux of the drive are directly controlled by inverter voltage space vector selection through a lookup table as shown in Table 1 [10]. The switching vectors to the inverter switches ( $T_1$ - $T_6$ ) are selected in such a way as to minimise flux and torque errors.

A PI speed regulator with limiter is used to generate reference torque  $T_e^*$ .

$$T_{e(n)}^* = T_{e(n-1)}^* + K_{pw} \left\{ \omega_{e(n)} - \omega_{e(n-1)} \right\} + K_{iw} \omega_{e(n)} \quad (9)$$

where  $\omega_e$  is the speed error (i.e.  $\omega_r^* - \omega_r$ ). Similarly, tuning of  $K_{pw}$  and  $K_{iw}$  are carried out using Ziegler Nichols method as mentioned above. The integral anti-windup is taken care of by back-calculation method.

Reference stator flux  $\psi_s^*$  is generated according to the sensed speed ( $\omega_r$ ) using flux computation block. Below the base speed the reference flux is equal to rated flux and the above base speed the reference flux is proportionately

**Table 1** Inverter voltage switching for DTC IM drive

$H_{\psi}$	$H_{T_e}$	S(1)	S(2)	S(3)	S(4)	S(5)	S(6)
1	1	V2(110)	V3(010)	V4(011)	V5(001)	V6(101)	V1(100)
	0	V7(000)	V8(111)	V7	V8	V7	V8
-1	-1	V6	V1	V2	V3	V4	V5
	1	V3	V4	V5	V6	V1	V2
	0	V8	V7	V8	V7	V8	V7
	-1	V5	V6	V1	V2	V3	V4

weakened as a function of rotor speed.

$$\psi_s^* = \psi_{s\_rated} \quad \text{for } \omega_r < \omega_{br} \quad (10)$$

$$\psi_s^* = \psi_{s\_rated} (\omega_{br} / \omega_r) \quad \text{for } \omega_r > \omega_{br} \quad (11)$$

where  $\psi_{s\_rated}$  is the rated flux,  $\omega_{br}$  is the base speed of the motor.

The reference stator flux  $\psi_s^*$  and torque  $T_e^*$  magnitudes are compared with the respective estimated values ( $\psi_s$ ,  $T_e$ ), and the errors are processed through hysteresis-band controllers as shown in Fig. 1 (DTC controller). The flux hysteresis controller is as follows

$$H_{\psi} = 1 \quad \text{if } |\psi_s^*| - |\psi_s| > +HB_{\psi_s} \quad (12)$$

$$H_{\psi} = -1 \quad \text{if } |\psi_s^*| - |\psi_s| < -HB_{\psi_s} \quad (13)$$

The torque hysteresis controller is given as

$$H_{T_e} = 1 \quad \text{if } |T_e^*| - |T_e| > +HB_{T_e} \quad (14)$$

$$H_{T_e} = -1 \quad \text{if } |T_e^*| - |T_e| < -HB_{T_e} \quad (15)$$

$$H_{T_e} = 0 \quad \text{if } -HB_{T_e} < (|T_e^*| - |T_e|) < +HB_{T_e} \quad (16)$$

where  $HB_{\psi_s}$  and  $HB_{T_e}$  are the flux and torque predefined hysteresis bands.

The actual stator flux  $\psi_s$  and electromagnetic torque  $T_e$  are estimated by using  $v_{dss}$ ,  $v_{qss}$  and  $i_{dss}$ ,  $i_{qss}$  (stator direct and

quadrature axes terminal voltages and currents) as

$$\psi_{ds} = \int (v_{dss} - i_{dss}R_s) dt + \psi_{ds0} \quad (17)$$

$$\psi_{qs} = \int (v_{qss} - i_{qss}R_s) dt + \psi_{qs0} \quad (18)$$

The flux is computed as

$$\psi_s = \sqrt{\psi_{ds}^2 + \psi_{qs}^2} \quad (19)$$

The developed torque is estimated as

$$T_e = (3/2)(P/2)(\psi_{ds}i_{qss} - \psi_{qs}i_{dss}) \quad (20)$$

where  $R_s$  is the stator resistance,  $\psi_{ds0}$  and  $\psi_{qs0}$  initial stator  $dq$  axes fluxes.

Considering  $d$ -axis is aligned with the  $a$ -axis, the three-phase voltages  $v_{abc}$  are transformed into stationary  $dq$  reference frame voltages ( $v_{dss}$  and  $v_{qss}$ ) by using Clarke transformation as

$$v_{dss} = (1/3)(2v_a - v_b - v_c) = v_a \quad (21)$$

$$v_{qss} = (1/3)(\sqrt{3}v_b - \sqrt{3}v_c) \quad (22)$$

The stator phase voltages  $v_{abc}$  are determined by the inverter

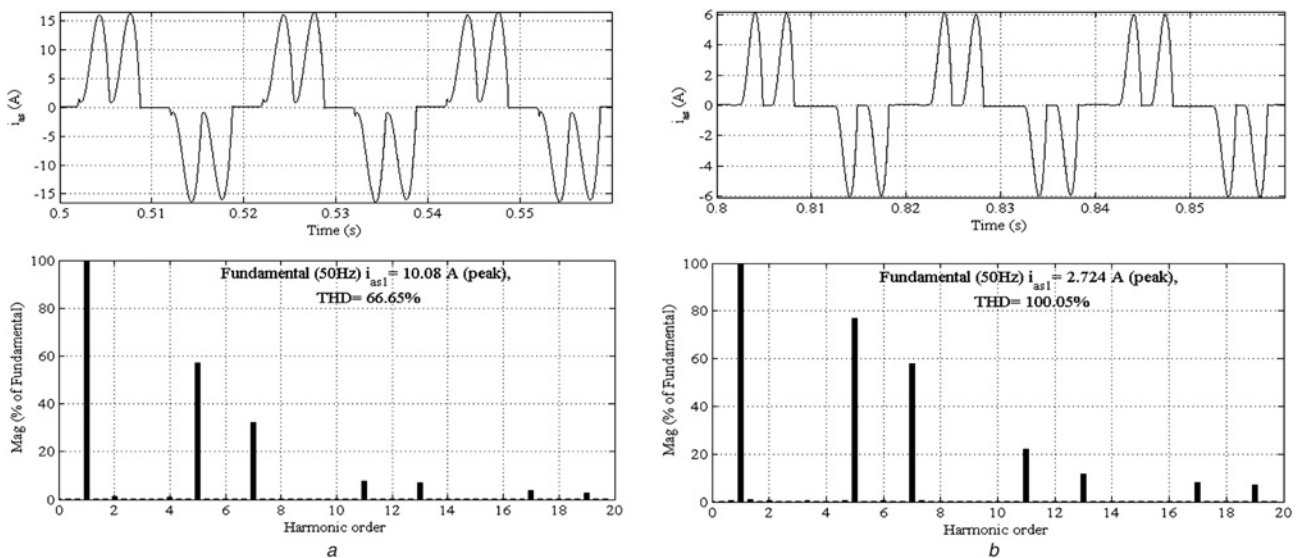


**Fig. 2** Harmonic spectrum of source current for simple DBR-fed DTC-based IMD at

- a Full load torque (100%)
- b Light load torque (20%)

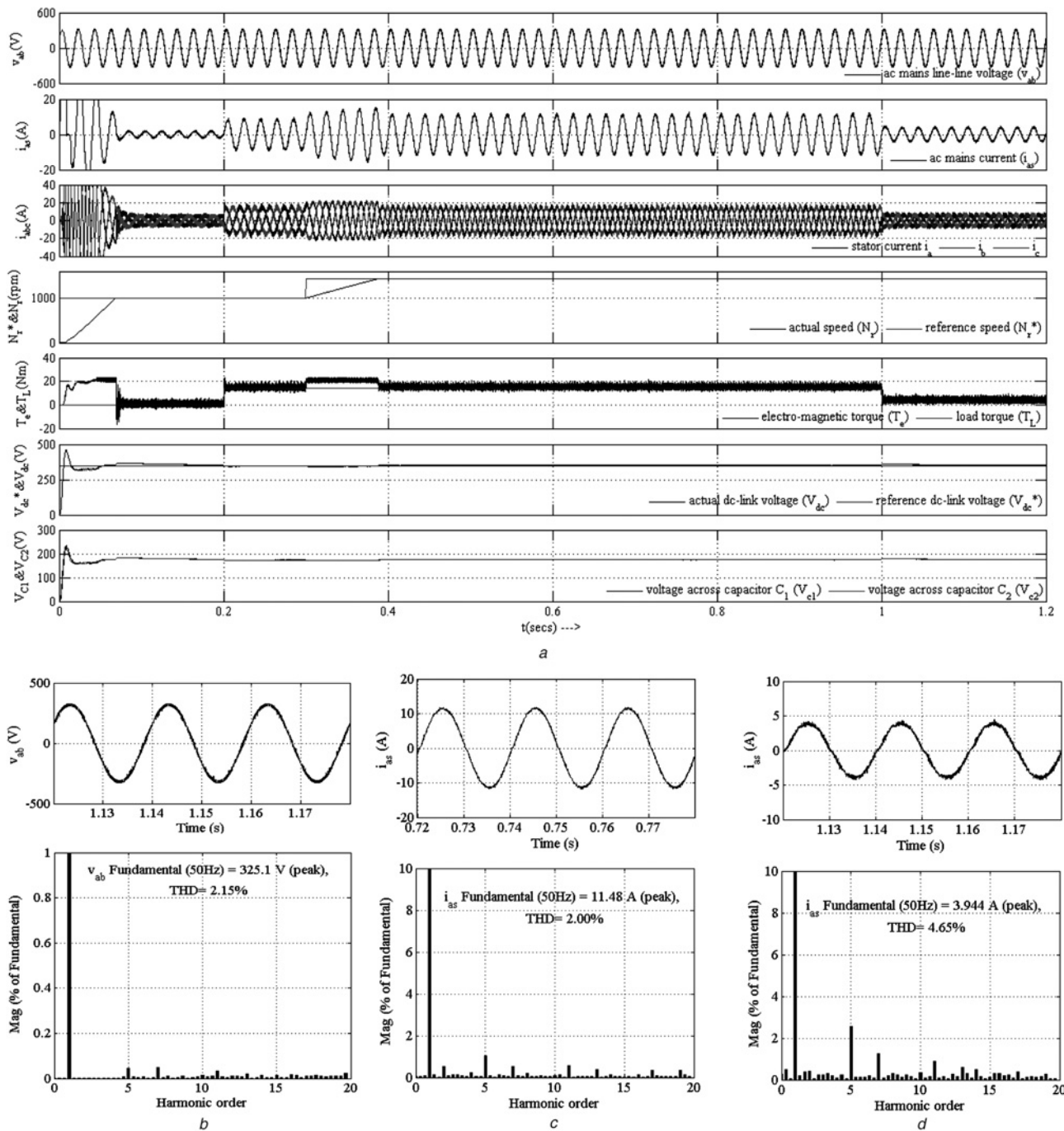


**Fig. 3** Dynamics and harmonic spectrum of the DTC-based IMD with a Vienna rectifier at the front end

- a Dynamics of Vienna rectifier fed DTC-based IMD
- b THD of ac mains line-line voltage at light load torque (20%)
- c THD of source current at full load torque (100%)
- d THD of ac mains current at light load torque (20%)

switching states ( $S_1, S_2$  and  $S_3$ ) and sensed dc-link voltage  $V_{dc}$  using the following equations

$$v_a = (V_{dc}/3)(2S_1 - S_2 - S_3) \quad (23)$$

$$v_b = (V_{dc}/3)(-S_1 + 2S_2 - S_3) \quad (24)$$

$$v_c = (V_{dc}/3)(-S_1 - S_2 + 2S_3) \quad (25)$$

Similarly, three-phase currents  $i_{abc}$  are also transformed into two-phase  $i_{dss}$  and  $i_{qss}$  using the above equation as

$$i_{dss} = (1/3)(2i_a - i_b - i_c) = i_a \quad (26)$$

$$i_{qss} = (1/3)(\sqrt{3} i_b - \sqrt{3} i_c) \quad (27)$$

where  $i_a$  and  $i_b$  are the sensed stator currents;  $i_c = -(i_a + i_b)$ .

### 3 MATLAB simulation

The performances of an un-controlled DBR-fed DTC-based IMD and Vienna rectifier-fed DTC-based IMD are

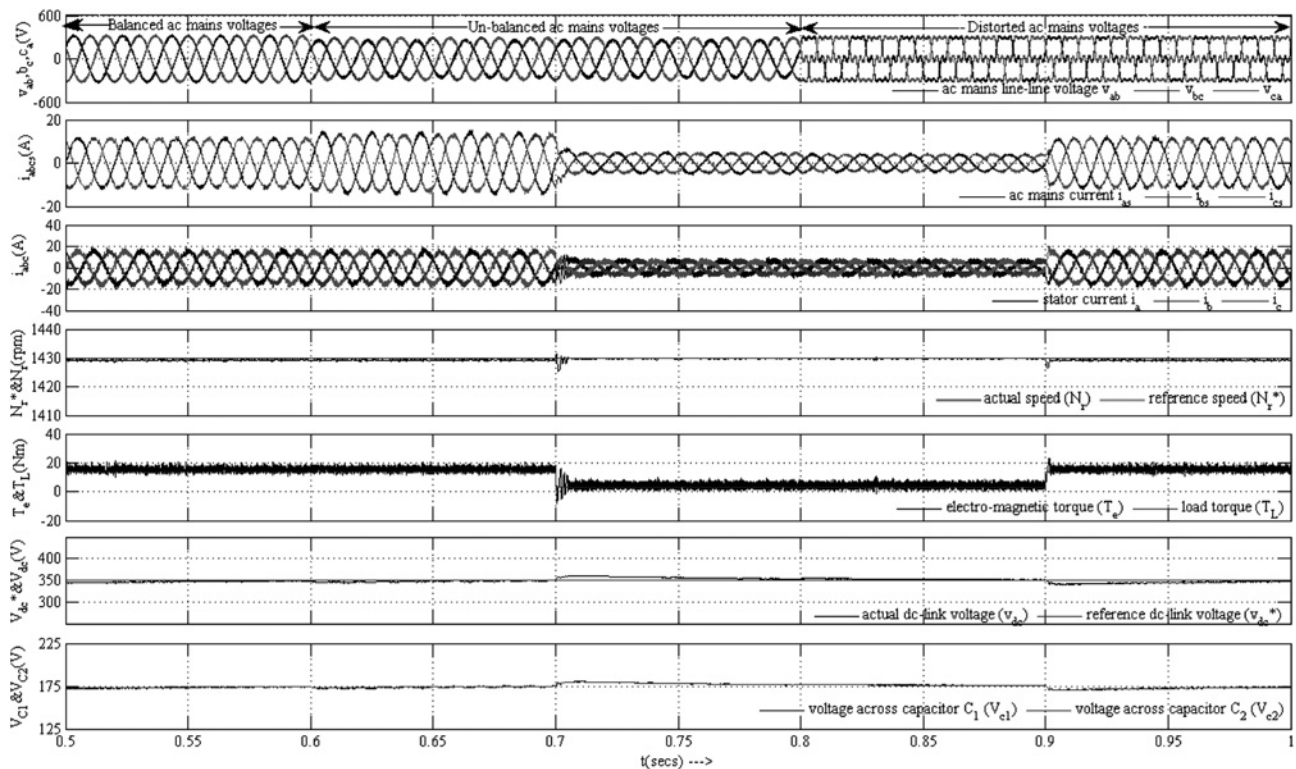


Fig. 4 Dynamics of Vienna rectifier fed DTC based IMD under balanced, un-balanced and distorted ac mains voltages

simulated using MATLAB software. Simulink and SimPowerSystems block sets are used for implementing the proposed drive system. The performances of these systems are studied for different operating conditions. A simulink model of DTC-based IMD with a conventional un-controlled six-pulse DBR at the front end is developed; subsequently, DBR is replaced by a Vienna rectifier for improving the power quality at the ac mains. The simulation is carried out for a three-phase 230 V, 50 Hz, 4-pole, 2.2 kW induction motor.

Fig. 2a shows the Fast Fourier Transformation (FFT) analysis of source current ( $i_{as}$ ) at full load torque (100%) with conventional un-controlled DBR-fed DTC-based IMD. It may be noted that with a simple DBR, the ac mains current waveform is highly non-sinusoidal because of which its THD is 66.65% at full-load. For 20% load torque, ac mains current THD is noted as 100.5% which is shown in Fig. 2b. Performance of the proposed Vienna rectifier-fed DTC-based IMD is tested for different perturbations like step increase/decrease in reference speed ( $N_r^*$ ) and step increase/decrease in load torque ( $T_L$ ). It is also analysed for non-ideal ac mains voltages (distorted and un-balanced). Fig. 3a shows the dynamics of the DTC-based IMD with a Vienna rectifier at the front end. Waveforms consist of ac mains line-line voltage ( $v_{ab}$ ), ac mains line current ( $i_{as}$ ), stator currents ( $i_{abc}$ ), rotor speed ( $N_r$ ), electromagnetic torque ( $T_e$ ),  $V_{dc}$  and  $V_{c1}$ ,  $V_{c2}$ . The motor is started at no-load with a reference speed of  $N_r^* = 1000$  rpm. The motor starts from zero speed and reaches 1000 rpm in about 73 ms. It can be seen that as the motor speeds up, the frequency of stator currents increases. The output of Vienna rectifier ( $V_{dc}$ ) reaches its reference value of 350 V in two power frequency cycle. At 0.2 s the load torque  $T_L$  is varied from no-load to full load torque of 14 Nm (100%). Sudden application of the load torque causes a momentary drop in rotor speed and the output of PI speed controller rises up

and hence increases the reference torque, thus increasing the developed torque ( $T_e$ ) causing the motor speed to settle at its reference value with the increased winding currents as shown in Fig. 3a. The dc-link voltage drops as the motor is loaded suddenly and the controller of the Vienna rectifier brings back  $V_{dc}$  to 350 V with power factor correction at the ac mains. At 0.3 s, the reference speed is increased from 1000 to 1430 rpm (rated). It can be observed that as the speed increases the frequency of stator currents increases. The load torque is reduced at 1 s from 14 to 2.8 Nm (20%) at a reference speed of 1430 rpm. Sudden removal of the load torque from the shaft causes an increase in rotor speed momentarily and the output of PI speed controller decreases the reference torque, thus decreasing the developed torque ( $T_e$ ) causing the motor speed to decrease and it settles at its reference value with appropriate variation in currents as shown in Fig. 3a. As the load torque is reduced the dc-link voltage increases and the controller of the Vienna rectifier acts on  $V_{dc}$  and it settles to its reference value.

THD of source phase voltage  $v_{as}$  at 20% load torque is shown in Fig. 3b. The ac mains current THD reduces to 2.0% at full load torque and 4.65% at 20% load torque by replacing this DBR with a Vienna rectifier as shown in Figs. 3c and d. It is also noted that the power factor is improved from 0.8 to 0.9998 at 100% load torque and 0.69 to 0.9850 at 20% load torque.

Fig. 4 shows the dynamics of the drive system for un-balanced and distorted ac mains voltages. At 0.6 s the ac mains phase voltages  $v_{as}$  and  $v_{bs}$  are reduced by 20%. At 0.7 s, the load torque is reduced from 100 to 20% and again increased to 100% at 0.9 s. Lower order harmonics (5th and 7th) are introduced into the ac mains voltages at 0.8 s. It is clearly shown that even when the supply voltage source is un-balanced and distorted the ac mains currents ( $i_{as}$ ,  $i_{bs}$  and  $i_{cs}$ ) are maintained balanced and sinusoidal. The THD of all three-phase source currents at 100% load torque

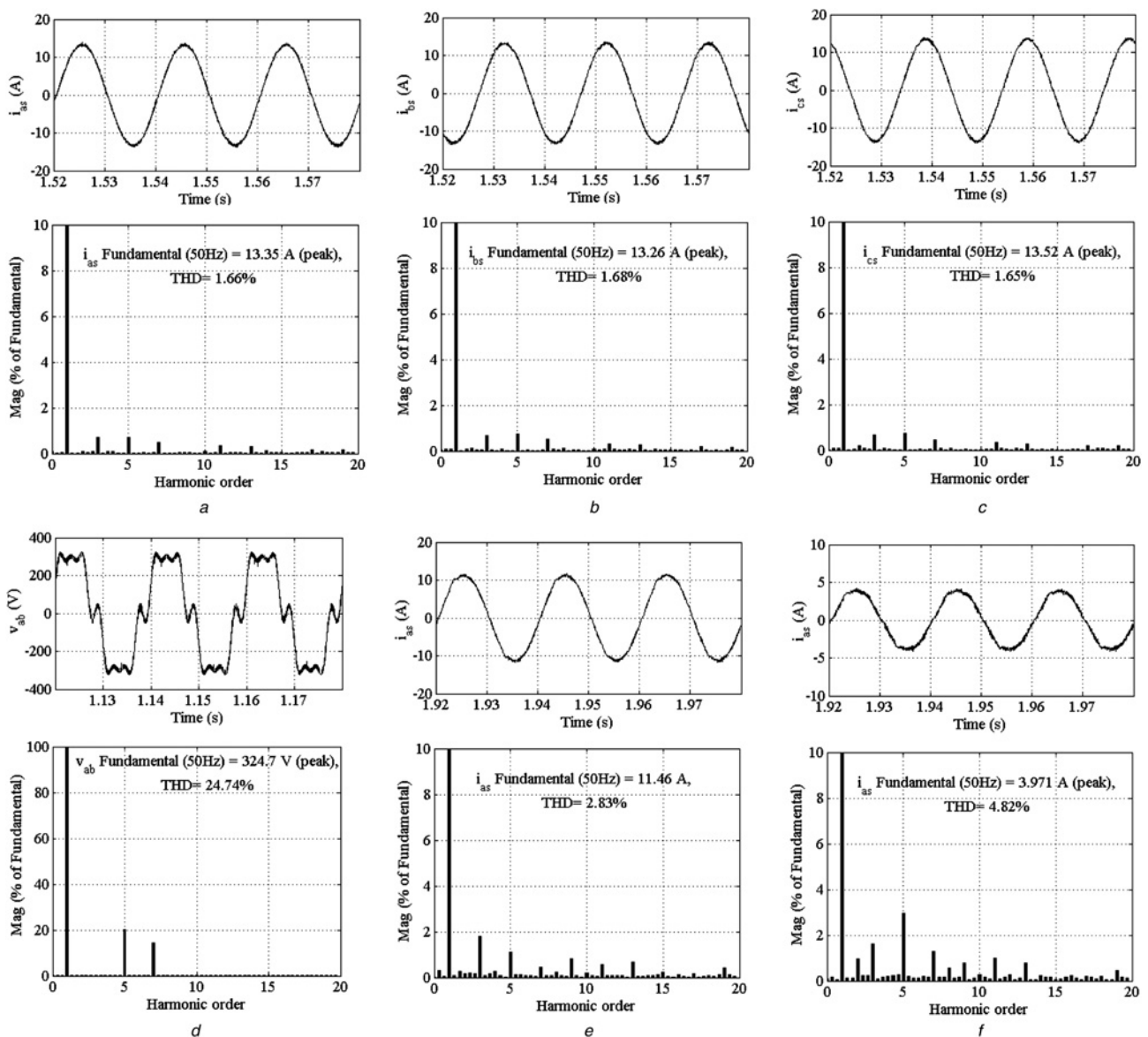
for un-balanced ac mains voltages are shown in Figs. 5a–c. It shows in Fig. 5d that the ac mains voltage is clearly distorted having a THD content of 24.74% and despite the ac mains currents are balanced sinusoids. THDs of ac mains currents and voltages at 100 and 20% load torques for distorted ac mains voltage are shown in Figs. 5e and f, respectively.

Fig. 6 shows a comparison between THD (%) at different load torques (%) for simple DBR and a Vienna rectifier fed DTC-based IMD. The PF against load torque (%) shown here despite that PF is maintained at unity. Comparison of different power quality indices of a simple DBR with a Vienna rectifier-fed DTC-based IMD is shown in Table 2. The harmonic performance of the Vienna rectifier with DTC-based IMD for three different conditions like balanced sinusoidal, un-balanced sinusoidal and distorted ac mains voltages are given in Table 2. Table 3 shows the comparison of different power quality indices of Vienna rectifier-fed DTC-based IMD at different load torques (%).

Based on these results it can be concluded that with a Vienna rectifier, the power quality indices have improved significantly and are well within IEEE-519 limit [11].

#### 4 Hardware implementation

The proposed drive system is experimentally verified by implementing it using DSP. The hardware interfacing block diagram with DSP is shown in Fig. 1. Texas Instrument's TMS320F2812 DSP [12] having 150MIPS processing speed, 16 twelve-bit analogue to digital conversion (ADC) channels and 16 PWMs is extremely suitable for motor control applications. Both DTC and Vienna rectifier control algorithms are implemented on this DSP. MATLAB real time workshop is used for developing the code composer studio code from the MATLAB/simulink model. Target support package block sets are used for developing the



**Fig. 5** Harmonic spectrum of all three-phase source currents and line-line voltages at 100% and 20% load torque for un-balanced and distorted ac mains voltages

- a–c THD of source currents ( $i_{as}$ ,  $i_{bs}$ ,  $i_{cs}$ ) at full load torque under un-balanced (20%) ac mains voltages
- d THD of distorted ac mains voltage at light load torque (20%)
- e THD of ac mains current ( $i_{as}$ ) at full load torque under distorted source voltages
- f THD of ac mains current ( $i_{as}$ ) at light load torque (20%) under distorted source voltages

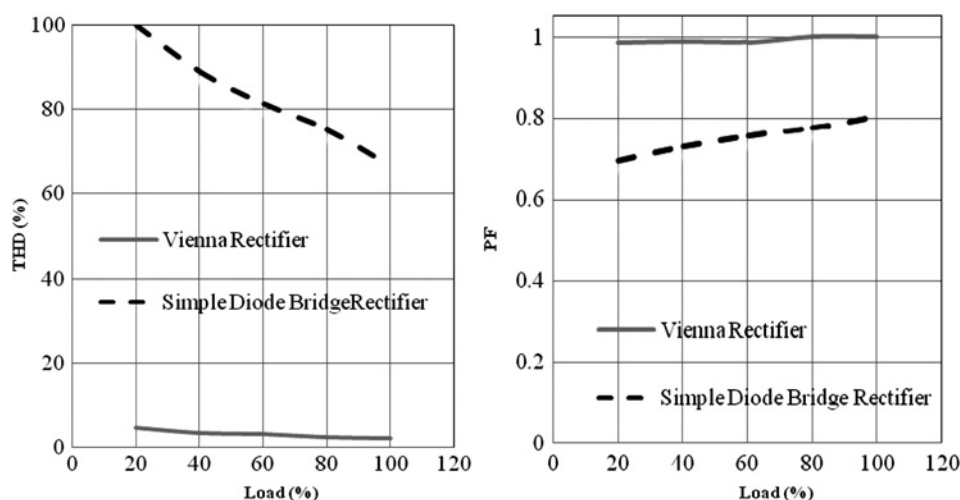


Fig. 6 THD (%) and PF with the load torque (%) for DTC-based IMD with Vienna rectifier and simple DBR

Table 2 Comparison of different power quality indices of a DTC-based IMD with different converters

Topology	THD (%) $v_{as}$ FL	$i_{as}$ THD, %		$i_{as,rms}$ (A)		DF		DPF		PF		$V_{dc}$ (V)	
		Full load	Light load (20%)	Full load	Light load (20%)	Full load	Light load (20%)	Full load	Light load (20%)	Full load	Light load (20%)	Full load	Light load (20%)
simple DBR	4.51	66.65	100.05	8.57	2.73	0.83	0.71	0.970	0.985	0.8	0.69	305	314
Vienna rectifier with balanced sinusoid source	2.12	2.00	4.65	8.11	2.82	0.9996	0.9939	0.987	0.990	0.9998	0.9850	350	350
Vienna rectifier with un-balanced sinusoid source	3.46	1.66	4.07	9.46	3.305	0.9997	0.9987	0.983	0.986	0.9998	0.9853	350	350
Vienna rectifier with distorted source	24.78	2.83	4.82	8.106	2.808	0.9995	0.9975	0.9868	0.9909	0.9998	0.9885	350	350

Table 3 Comparison of different power quality indices of a DTC-based IMD with Vienna rectifier

Load, %	THD, %		Crest factor of $i_{as}$	DF	DPF	PF	$V_{dc}$ (V)
	$i_{as}$	$v_{as}$					
20	4.65	2.10	1.418	0.9939	0.990	0.9850	350
40	3.43	2.15	1.414	0.9982	0.989	0.9870	350
60	3.06	2.20	1.372	0.9985	0.988	0.9880	350
80	2.27	2.04	1.406	0.9994	0.987	0.9997	350
100	2.00	2.12	1.416	0.9996	0.987	0.9998	350

control algorithm. Vienna rectifier switches are controlled in such a way that it should maintain dc-link voltage at the regulated value, balanced capacitor voltage, UPF and sinusoidal currents at ac mains. The output of the Vienna rectifier is connected to the three-phase VSI through two-capacitors. The pulses to the VSI which drives the three-phase induction motor are generated using DTC algorithm. A 230 V, 2.2 kW, 4-pole, 50 Hz, three-phase induction motor is used for the hardware implementation.

Figs. 7a–d show the experimental results of the proposed Vienna rectifier-fed DTC-based IMD performance during speed transients, load torque transients and steady state conditions. Fig. 7a shows the dynamics of the proposed Vienna rectifier-fed DTC-based IMD during starting. The motor is started at 35% load torque with a reference speed

of  $N_r^* = 1000$  rpm. The motor starts from 0 speed and reaches 1000 rpm at about 0.1 s. It can be seen that as the motor speeds up, the frequency of the stator currents increases. The output voltage of the Vienna rectifier ( $V_{dc}$ ) is regulated to its reference value ( $V_{dc}^*$ ) of 350 V. Fig. 7b shows that as the speed increases from 1200 to 1430 rpm at rated load torque the frequency of the stator currents increases. Fig. 7c shows the stator current ( $i_{bs}$ ), rotor speed ( $N_r$ ), dc-link voltage ( $V_{dc}$ ) and mid-point dc-link voltage ( $V_{c2}$ ) waveforms for a step increase in the load torque on the motor from 8.4 Nm to rated load torque (14 Nm) at rated speed (1430 rpm). Sudden application of the load torque causes a momentary drop in the rotor speed and the output of the PI speed controller increases the reference torque, thus increasing the developed torque ( $T_c$ ). Thus, the

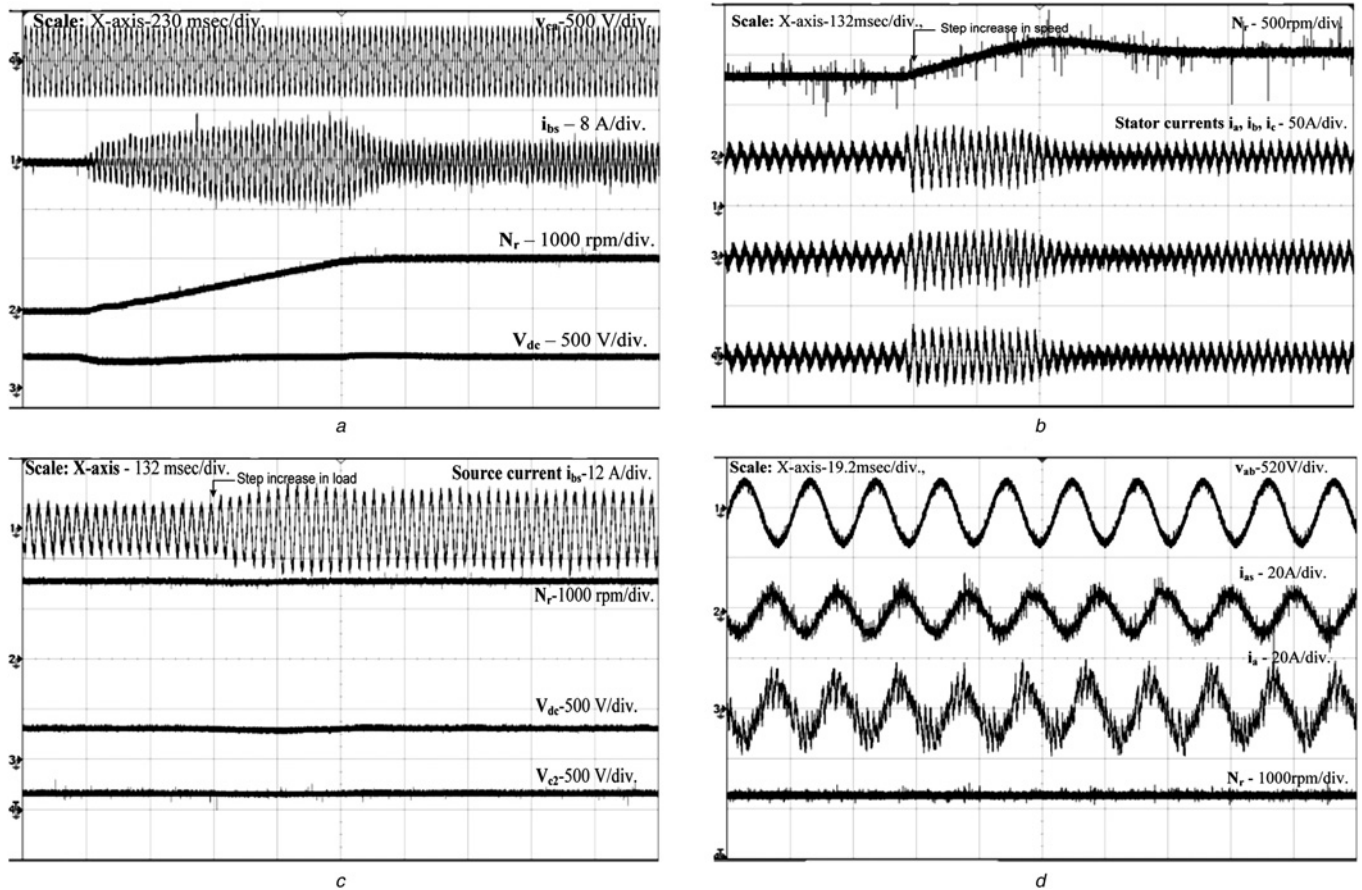


**Fig. 7** Experimental results of the proposed Vienna rectifier-fed DTC-based IMD performance during starting, speed transients, load torque transients and steady state conditions

- a Dynamics during starting at  $N_r^* = 1000$  rpm and 5 Nm load torque
- b Step increase in reference speed from 1200 rpm to 1430 rpm at rated load torque
- c Step increase in load torque from 8.4 to 14 Nm at  $N_r^* = 1430$  rpm and  $V_{dc}^* = 350$  V
- d Steady-state waveforms at rated-load torque and rated speed

motor speed settles at its reference value with the increased winding currents. The load torque on induction motor is varied by loading DC generator which is coupled to the induction motor. As the load torque increases the dc-link voltage and mid-point dc-link voltages are seeing a small drop and the output of PI controller increases the reference dc current, thus stabilising the dc-link voltage to its reference value. Mid-point dc-link voltage PI controller is used for balancing the voltages across the two capacitors ( $C_1$  and  $C_2$ ). It is clearly shown in Fig. 7c that the second capacitor voltage ( $V_{c2}$ ) is exactly half of the actual dc-link voltage, thus both capacitor voltages are balanced. Steady state waveforms of ac mains line-line voltage ( $v_{ab}$ ), ac mains current ( $i_{as}$ ), stator current ( $i_a$ ) and speed ( $N_r$ ) at rated-load torque of 14 Nm and rated speed of 1430 rpm are shown in Fig. 7d. It is clearly visible that the ac mains current is nearly sinusoidal.

Figs. 8a and b show the mains line-line voltage ( $v_{ca}$ ), ac mains line current ( $i_{bs}$ ) and its power. The THD of source current ( $i_{bs}$ ) and line-line voltage ( $v_{ca}$ ) at the rated load torque and rated speed for the Vienna rectifier-fed DTC-based IMD are shown in Figs. 8c and d. From the simulated and experimental results, it is very evident that the use of a Vienna rectifier has significantly improved the power quality at the front end as compared with the case with a six-pulse DBR. The input current THD has come down from the original value of 66% (in the case of an uncontrolled

converter) to  $< 5\%$  in the case of a Vienna rectifier. In all, it is very clear that Vienna rectifier has enhanced the power quality of the DTC-based IMD remarkably at the PCC.

## 5 Conclusion

The power quality problems in a conventional un-controlled six-pulse DBR-fed DTC-based IMD have been mitigated using a three-phase Vienna rectifier in this work. It has been shown that by employing an improved power quality converter known as Vienna rectifier, sinusoidal input currents have been achieved with power factor correction and dc-link voltage regulation. This improved power quality converter has used only three active switches for a DTC-based IMD for improving the power quality at the utility interface. The performance of the proposed system has been analysed for unbalanced and distorted ac mains voltages, load torque and speed perturbations. The proposed system, that is, Vienna rectifier-fed DTC-based IMD has been experimentally validated by implementing a prototype of 2.2 kW rating. The Vienna rectifier controller and DTC controller have been developed using DSP. The developed DTC-IM drive with a Vienna rectifier have improved the ac mains current THD, power factor and other power quality indices which are well within IEEE-519 standard limit during wide range of load variations on the drive.

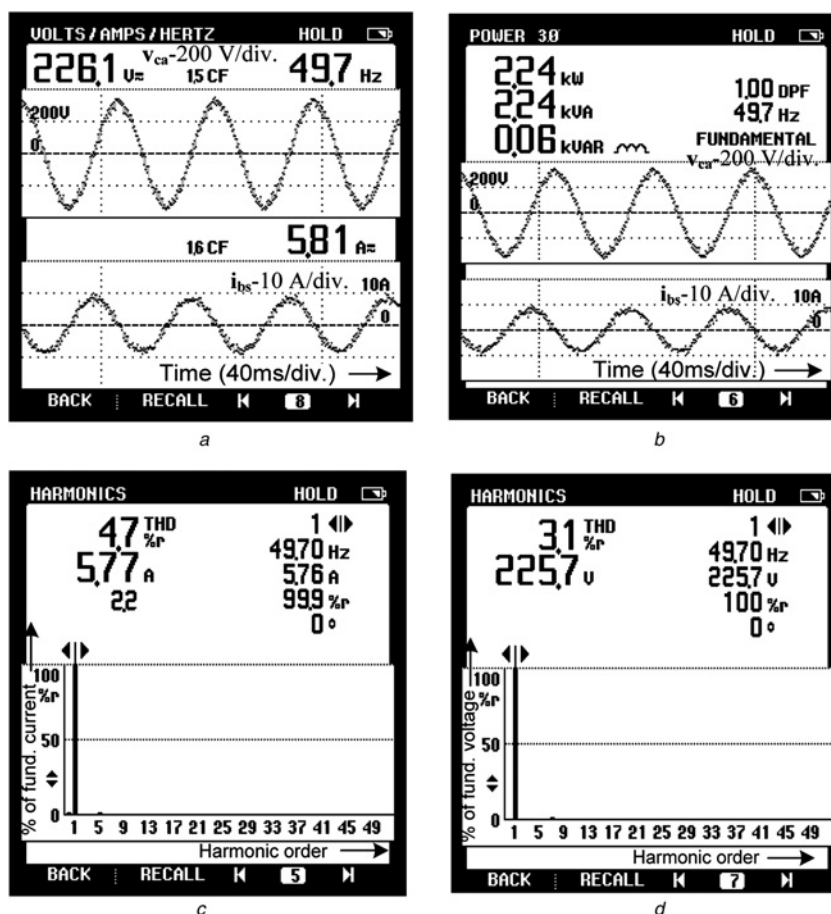


**Fig. 8** Experimental results of Vienna rectifier fed DTC-based IMD at rated load torque and rated speed

- a  $v_{ca}$  and  $i_{bs}$   
 b AC mains power  
 c  $i_{bs}$  THD  
 d  $v_{ca}$  THD

## 6 References

- Singh, B., Bhuvanawari, G., Garg, V.: 'Harmonic mitigation in AC–DC converters for vector controlled induction motor drives', *IEEE Trans. Energy Convers.*, 2007, **22**, (3), pp. 637–646
- Domenico Casadei, B., Profumo, F., Serra, G., Tani, A.: 'FOC and DTC: two viable schemes for induction motors torque control', *IEEE Trans. Power Electron.*, 2002, **17**, (5), pp. 779–787
- Domijan Jr., A., Embriz-Santander, E.: 'Harmonic mitigation techniques for the improvement of power quality of adjustable speed drives (ASDs)'. Proc. IEEE Applied Power Electronics Conf. and Exposition, *APEC'90*, March 1990, pp. 96–105
- Singh, B., Singh, B.N., Chandra, A., Al-Haddad, K., Pandey, A., Kothari, D.P.: 'A review of three-phase improved power quality AC-DC converters', *IEEE Trans. Ind. Electron.*, 2004, **51**, (3), pp. 641–660
- Kolar, J.W., Ertl, H., Zach, F.C.: 'Design and experimental investigation of a three-phase high power density high efficiency unity power factor PWM (VIENNA) rectifier employing a novel integrated power semi-conductor module'. Proc. IEEE APEC'96, 1996, pp. 514–523
- Kolar, J.W., Ertl, H., Zach, F.C.: 'A novel three-phase utility interface minimizing line current harmonics of high-power telecommunications rectifier modules'. Proc. 16th Int. Telecommunications Energy Conf. INTELEC '94, 1994, pp. 367–374
- Dalessandro, L., Drogenik, U., Round, S.D., Kolar, J.W.: 'A novel hysteresis current control for three-phase three-level PWM rectifiers', *Applied Power Electronics Conf. and Exposition*, 2005, **1**, pp. 501–507
- Bel Hadj-Youssef, N., Al-Haddad, K., Kanaan, H.Y., Fnaiech, F.: 'Small-signal perturbation technique used for DSP-based identification of a three-phase three-level boost-type Vienna rectifier', *IET, Electr. Power Appl.*, 2007, **1**, (2), pp. 199–208
- Naik, R., Rastogi, M., Mohan, N.: 'Third-harmonic modulated power electronics interface with 3-phase utility to provide a regulated DC output and to minimize line-current harmonics'. Proc. IEEE Conf. on Industry Applications Society Annual Meeting, October 1992, vol. 1, pp. 689–694
- Bose, B.K.: 'Modern power electronics and AC drives' (Pearson Prentice Hall, 2007, 4th edn.)
- IEEE Recommended Practices and Requirements for Harmonic Control in Electrical Power Systems, IEEE Standard 519–1992
- Texas Instruments Application Notes, 'TMS320F2812 Digital Signal Processor-Implementation Tutorial'. DSP28
- Rashid, M.H.: 'Power electronics-circuits, devices and applications' (Pearson Prentice Hall, 2009, 4th edn.)

## 7 Appendix

*Motor specifications:* three-phase, 3 hp (2.2 kW) squirrel cage induction motor, four-pole, 1430 rpm, 230 V, 50 Hz, Y-connected, rated current = 8.3 A, 0.82 PF,  $R_s = 0.603 \Omega$ ,  $R_r = 0.7 \Omega$ ,  $X_{ls} = 1.007 \Omega$ ,  $X_{lr} = 0.9212 \Omega$ ,  $X_m = 23.56 \Omega$ ,  $J = 0.011 \text{ kg/m}^2$ .

*Vienna rectifier:* three IXYS VUM25-05E PFC modules are the building blocks for developing the three-phase Vienna rectifier power circuit.

$$V_{dc}^* = 350 \text{ V}$$

Boost inductance ( $L_b$ ) – it is designed by considering one phase, one inductor, one switch and one freewheeling diode combined

**Table 4** Current distortion limits for general distribution systems

Maximum harmonic current distortion in percent of $I_L$						
Individual harmonic order (odd harmonics)						
$I_{sc}/I_L$	< 11	$11 \leq h \leq 17$	$17 \leq h \leq 23$	$23 \leq h \leq 35$	$35 \leq h$	Total demand distortion
< 20	4.0	2.0	1.5	0.6	0.3	5.0
20 < 50	7.0	3.5	2.5	1.0	0.5	8.0
50 < 100	10.0	4.5	4.0	1.5	0.7	12.0
100 < 1000	12.0	7.0	6.0	2.5	1.4	20.0

Where:  $I_{sc}$  = maximum short-circuit current at PCC,  $I_L$  = maximum demand load current (fundamental frequency component) at PCC,  $h$  = harmonic order.

as a boost converter. The inductor is basically to provide the required voltage boost for a given peak–peak ripple ( $\Delta i_{LP}$ )

$$L_b = (V_{sph\_peak} \times D) / (f_{sw} \times \Delta i_{LP}) = 4 \text{ mH}$$

where  $V_{sph\_peak}$  = peak source phase to neutral voltage = 187.79 V

$$V_{in} = (2V_{sph\_peak}) / \pi = 215.72 \text{ V}, \quad V_{C1} = 350 \text{ V}$$

$$D = \text{duty ratio} = 1 - (V_{in} / V_{C1}) = 0.3168$$

$$f_{sw} = \text{switching frequency} = 20 \text{ kHz}$$

$\Delta i_{LP}$  = inductor peak ripple current =  $(2 \times P \times \% \text{ripple}) / V_{sph\_peak}$ , by considering 3% peak current ripple and 2.2 kW, then  $\Delta i_{LP} = 0.702 \text{ A}$

Boost capacitance – The capacitance is designed to maintain a constant dc-link voltage with 1.1% voltage ripple ( $\Delta V_{dc}$ )

$$C = I_{rated} / (6 \times \omega \times \Delta V_{dc}) = 8.3 / (6 \times 314 \times 4) = 1100 \mu\text{F}$$

$$C_1 = C_2 = 2C = 2200 \mu\text{F}$$

*Input:* 230 Vrms L–L, 50 Hz, source impedance  $Z_s = 0.5\%$  of base impedance  $Z_{base}$

*Voltage source inverter:* three-Phase 25 kVA, 750 V (DC) semikron inverter.

*Digital signal processor:* digital spectrum's make eZdsp F2812 (32-bit) having clock frequency of 150 MHz, two event managers (EVA and EVB) each event managers having two-general purpose timers, six-PWM channels, eight 12-bit ADC channels, three-capture units, three-quadrature-encoder pulse (QEP) channels.

*IEEE-519 limits [11]:* current distortion limits for general distribution systems (120 V through 69000 V), Table 4

*Different power quality indices are defined as follows [13]:* THD is a measure of closeness in shape between a waveform and its fundamental component.

Crest factor is a measure of the peak of the waveform as compared with its rms value.

DPF is a cosine of angle between the fundamental components of the input current and voltage.

Distortion factor is the the ratio of the rms of the fundamental component to the rms value of the entire waveform (fundamental + harmonics).